ELSEVIER

Thermochimica Acta 356 (2000) 85–96

thermochimica acta

www.elsevier.com/locate/tca

Qualitative and quantitative aspects of microwave thermal analysis

G.M.B. Parkes[a], P.A. Barnes[a,*], G. Bond[b], E.L. Charsley[c]

[a]*Centre for Applied Catalysis, Materials Research Division, University of Huddersfield, Queensgate, Huddersfield HD1 3DH, UK*
[b]*Centre for Materials Research, University of Central Lancashire, Central Lancashire PR1 3HE, UK*
[c]*Centre for Thermal Studies, Materials Research Division, University of Huddersfield, Huddersfield HD1 3DH, UK*

Received 1 November 1999; accepted 1 February 2000

Abstract

Thermally induced transformations in materials (e.g. melting, decomposition or solid–solid phase changes) alter their dielectric properties and hence their ability to interact with a microwave field. This paper describes a new technique, microwave thermal analysis, where microwaves are used both to heat a material and as a means of detecting thermal transitions. Two approaches are described. The first is based on the changes in the temperature of a material when subjected to a constant microwave power and the second on the microwave power profile obtained when a material is heated in a controlled (linear) manner. Both approaches can provide qualitative and quantitative information on solid state processes. A classification is proposed for the different types of results found for various materials and transitions. The advantages and limitations of studying transitions and reactions using microwave energy are discussed.

Keywords: Dielectric; Materials characterisation; Thermal analysis; MWTA

1. Introduction

Microwave thermal analysis (MWTA) has three potential advantages over conventional thermal analysis. Firstly, as the radiation is penetrative and heats by direct interaction it reduces the temperature gradients which are formed within a material when using conventional heating techniques, using furnaces, which depend upon conduction. This greater uniformity of heating can increase the resolution of thermal events which are adjacent in terms of temperature. Secondly, as the sample (and sample cell) effectively act as the furnace, the whole system has an intrinsically low thermal mass. Thirdly, and most importantly, MWTA provides a totally new means of studying thermal transitions, based upon changes in a material's dielectric properties, which is complementary to techniques such as differential scanning calorimetry (DSC) and thermogravimetry (TG).

In addition to providing a new approach to thermal analysis, the technique has considerable potential for investigating the interaction of microwaves with materials which is of particular value since microwave heating is becoming increasingly widely used in both chemical and materials science. It has been applied to areas as diverse as the pyrolysis of coals [1], the sintering of ceramics [2], the processing of polymers [3], the preparation of supported catalysts [4,5] and various drying applications [6,7]. Clearly, there is a need to develop an understanding of how changes in such materials affect their interaction with microwave energy.

* Corresponding author. Tel.: +44-1484-473-138; fax: +44-1484-472-182.

0040-6031/00/$ – see front matter
PII: S0040-6031(00)00458-5

1.1. Microwave heating in thermal analysis

The theory of microwave heating has been described in detail elsewhere [8] and only a brief overview is presented here. The extent to which a material is heated when subjected to microwave radiation depends on two critical parameters, the dielectric constant, ε', and the dielectric loss factor, ε'' of the material. The dielectric constant describes the ease with which a material is polarised by an electric field, while the dielectric loss factor measures the efficiency with which the electromagnetic radiation is converted into heat. The ratio of the two gives the *dielectric loss tangent*:

$$\tan\delta = \frac{\varepsilon''}{\varepsilon'}$$

which defines the ability of a material to absorb and convert electromagnetic energy into thermal energy. The factor $\tan\delta$ (sometimes called the *loss factor*, with materials possessing a degree of *lossiness*) is dependent on both the temperature and the frequency of the microwave radiation. The dielectric properties of a material are also dependent on its atomic/molecular geometry. Thus, alterations in molecular or structural rearrangement of a material (as found in decomposition, fusion and phase changes, etc.) affect $\tan\delta$, to a greater or lesser extent, and hence the degree to which the material is heated.

Most work to date investigating the effects of microwave heating has been performed with multimode cavities (where the wave is allowed to pass through the sample at different angles caused by random reflections from the cavity walls). These devices are functionally identical to ovens used for cooking and often have generators that can either only produce a fixed power level, or which use simple pulsed width modulation.

For thermal analysis applications, involving detailed studies of the effects of transitions in materials on dielectric properties, much greater control of the temperature is needed, requiring the use of sophisticated equipment and control systems. As a result, relatively little work has been undertaken in this field, apart from the work of Karmazsin et al., who first explored the potential of microwaves as a form of heating in thermal analysis [9,10].

1.2. Detection of thermal transitions via microwave heating

We have developed equipment [11] for studying the heating effects of microwave energy and the changes induced in this relationship by reactions and transitions in materials. Two principle modes for detecting these transitions are available using MWTA.

1.2.1. Mode 1

Either a constant or programmed, power is applied to the sample and the resultant time-temperature profile recorded. For constant power experiments, this mode is analogous to the conventional time-temperature profile obtained for a material placed in a constant temperature furnace. For an inert material the profile will be smooth, though non-linear, while for a material undergoing a transition resulting in a change in loss factor, a discontinuity will be produced. Other factors contributing to the overall shape of the profile include the heat capacity of the material and the enthalpy of any reactions or transitions, but these are often small in comparison to the effect of loss factor.

1.2.2. Mode 2

The sample is subjected to a linearly increasing temperature regime as typically used in conventional thermal analysis experiments. To achieve this it is necessary to continuously adjust the microwave power applied to the sample by the use of a feedback algorithm. For an inert material the resultant applied power profile is smooth, but non-linear, as the loss factor for most materials varies (often increasing) with temperature. For a material undergoing a thermal transition, any associated change in loss factor will necessitate an abrupt increase or decrease in the microwave power required to maintain the set heating rate. Such power changes appear either as a discrete step or a complex peak and form the basis of a novel means of detecting thermally induced transformations.

To aid the interpretation of results obtained using MWTA we have developed a classification of the main features in the power profiles obtained in linear heating (Mode 2) experiments based on the most frequently observed types which are illustrated schematically in Fig. 1.

Type I (Fig. 1a) consists of a discrete 'step' in the power profile as the material undergoes a transition

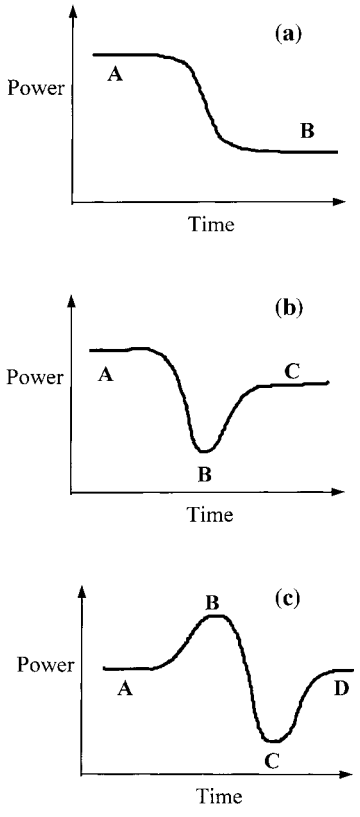

Fig. 1. Classification of the most common types of power profile observed for thermal transitions under linear heating conditions, (a) Type I. The power profile has a discrete 'step' with a difference in the level prior to the transition (A) and after the transition (B); (b) Type II. Similar to Type I, but with a distinct 'peak' (B) between the initial power level (A) and final level (C); (c) Type III. Consists of a distinct positive (A) and negative (B) peak between initial power level (A) and final level (D).

producing a change in loss factor. A negative step indicates that the loss factor has increased (i.e. less power is required to maintain the set heating rate) while a positive step indicates a decrease in loss factor.

Type II (Fig. 1b) consists of a distinct negative peak where the power falls to a minimum before rising again. This may be combined with an overall step change in the power profile as seen in Type I.

Type III (Fig. 1c) consists of a positive peak followed by a negative peak in the power profile. This may also be combined with an overall step change in the power profile.

For clarity, the figures show a horizontal power baseline before and after the transition. However, the changes in the profile are usually superimposed on an underlying sloping power baseline. In addition, the three basic types can be seen in combination.

2. Experimental

2.1. Instrumentation

The apparatus (Fig. 2), described in detail elsewhere [11], is based on a single mode system which is tuned to set up a standing wave with a maximum in the electric field component (E) coinciding with the location of the sample.

The microwave power, which can be varied in 1 W steps to 300 W, is supplied by a high stability, narrow-band 2.45 GHz generator (Sairem) under computer control. The microwaves are passed from the generator, via a water-cooled circulator used to absorb any reflected power, to a launcher incorporated into a brass waveguide (Type 340, internal dimensions 86 mm×43 mm). The sample is located in a section of the waveguide which has four circular ports, the two larger of which are vertical (diameter 50 mm) and allow insertion and removal of the sample cell, while the two smaller are horizontal (diameter 15 mm) and provide access for temperature measurement devices.

Tuning is provided by three components. Firstly, a 'short circuit' or 'plunge tuner' which can be used to alter the internal length of the waveguide, secondly, a variable iris, consisting of a thin copper sheet with a rectangular orifice (50 mm×25 mm) which can be traversed over a range of 6 cm, and thirdly an automated four-stub tuner. This latter device provides continuous 'fine-tuning' via the vertical movement of four brass rods in the waveguide and compensates for any small alterations in the system tuning produced by the sample and cell as they are heated.

2.2. Heating regimes

The MWTA instrument, utilising data acquisition and control software developed by the authors, supports a variety of microwave heating regimes including constant power (e.g. 150 W), programmed power (e.g. 2 W min^{-1} to 200 W) or linear heating (e.g. 5°C min^{-1} to 300°C). The first two methods

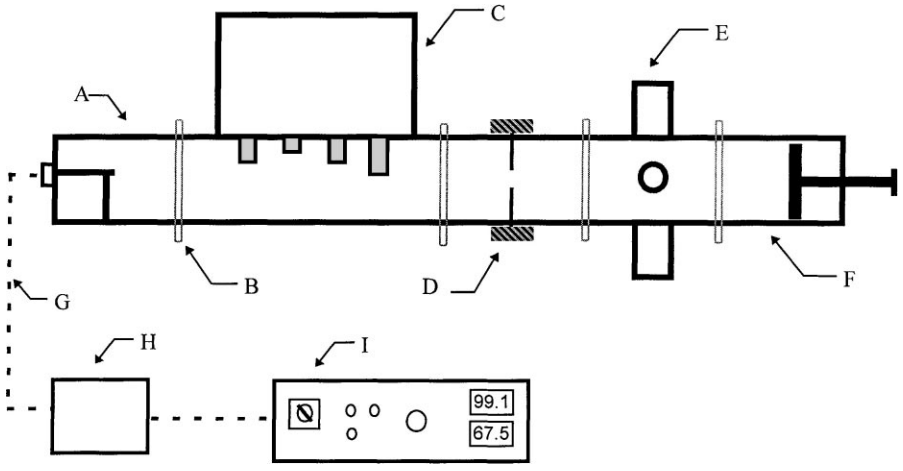

Fig. 2. Schematic diagram of the microwave components of the MWTA instrument. (A) Launch section of the waveguide, (B) waveguide flange connector, (C) four stub tuner, (D) variable iris, (E) sample section, (F) short circuit tuner, (G) microwave power cable, (H) water-cooled dummy load, (I) variable power generator.

provide information from the temperature–time profile (Mode 1) while the latter provides information from the power–time or power–temperature profile (Mode 2).

In addition to the three basic types of experiment described above, more complex strategies involving modulation of the forward power are possible including fixed amplitude power or temperature modulations. Differential techniques where the temperature of the sample is compared with that of an inert reference material are also possible and are described in detail elsewhere [12].

2.3. Temperature measurement

The accurate measurement of the sample temperature is crucial in thermal studies. Metal objects, including wires, cannot normally be placed in a microwave field without either severely distorting it or causing electrical discharges. However, in confirmation of the findings of Karmazsin et al. [13] and others, we have found that it is possible to use thermocouples in a waveguide provided they are thin, have a grounded metal sheath and are held exactly at 90° to the electric field component of the microwave energy [14]. For the present study, 0.5 mm diameter, stainless steel sheathed type K (chrome-alumel) thermocouples (Omega Engineering) were used, covering a temperature range from 0 to 1000°C.

2.4. Sample cell designs

A variety of sample cells have been developed for use in the MWTA instrument, their design and construction being largely determined by the quantity of material to be analysed and the type of experiment to be undertaken. Typically, the cells have been constructed from either boro-silicate or silica glass, depending on the temperature range used, or a combination of ceramic tubing (alumina) and alumino-silicate cement. They are generally designed to have a high degree of symmetry to prevent uneven distortions of the microwave field. Schematic diagrams of the MWTA cells used in the current work are shown in Fig. 3.

Fig. 3a shows the simplest cell design (Cell A) comprising a glass tube (6 mm o.d., 1 mm wall thickness) with a central spherical bulb. The cell has a total length of 300 mm and a range of sizes has been constructed with bulb diameters between 10 and 20 mm to contain sample masses of ca. 500–1000 mg. The bulb has a thin-walled well of depth half the bulb diameter and of a bore sufficient to contain the 0.5 mm thermocouple.

Fig. 3b shows a cell design that incorporates two main components, the main body of the cell and a

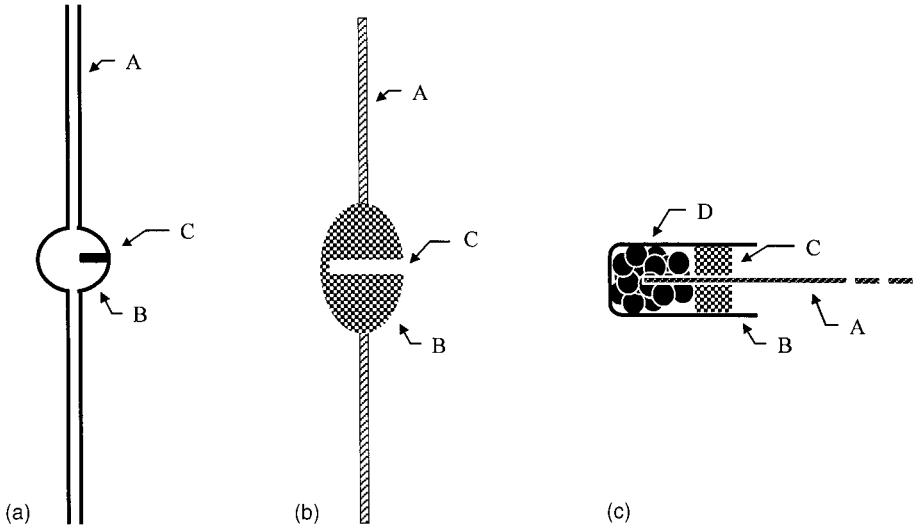

Fig. 3. (a) Schematic diagram of basic MWTA cell (Cell A). (A) 6 mm o.d. glass tube; (B) sample bulb; (C) well for thermocouple; (b). Schematic diagram of body of removable holder cell (Cell B). (A) ceramic stem; (B) aluminosilicate body; (C) inlet for removable sample holder; (c) schematic diagram of sample holder for Cell B. (A) thermocouple; (B) 6 mm o.d. silica cup; (C) ashing mat plug; (D) sample.

removable sample holder (Cell B). The body of the cell comprises a ceramic tube (alumina, length 300 mm, o.d. 6 mm) supporting an ovoid construction (height 60 mm, width 45 mm) made from a mixture of high temperature alumino-silicate cement and silicon carbide fired at 800°C. Into this body a hole is inlet, (depth 20 mm, diameter 8 mm) designed to accommodate the removable sample holder (Fig. 3c). The cell body has a mass of approximately 50 g. The sample holder comprises a silica tube (length 20 mm, o.d. 8 mm, i.d. 6 mm, mass 1 g) sealed at one end which can be simply inserted and removed from the cell body. It can accommodate samples with masses between 100 and 400 mg, depending on the density of the materials in question.

The design of Cell A means that it does not contribute significantly to the heating of the sample as the silica glass used in its construction is almost transparent to microwave radiation. The incorporation of alumino-silicate cement mixed with silicon carbide in Cell B increases the mass of microwave susceptible material present and provides a supplementary heat source for the smaller volume samples used with this cell, which is of particular importance for materials with a low dielectric loss factor.

2.5. Sample preparation

In many instances materials can be used directly, but in some MWTA experiments it is often desirable to mix the sample with another solid for four main reasons:

1. To increase the overall volume of the sample to ensure sufficient direct coupling with the microwave field.
2. To provide sufficient volume of material to permit the thermocouple to be accurately positioned for good temperature measurement.
3. To introduce a material which acts as a ‘susceptor’ to provide an intimate source of ‘internal’ heating for materials which only poorly absorb microwave energy [15].
4. To dilute materials which interact strongly with microwave energy.

Two solid additives were used in the current work. The first, silicon carbide (Aldrich 400 mesh), is chemically inert over a wide temperature range, is a strong absorber of microwave energy [16,17] and has a high thermal conductivity [18]. The second, alumina (Aldrich 400 mesh, calcined at 800°C for

3 h), also has a low chemical reactivity but is a relatively weak absorber of microwave energy.

3. Results

The materials used in this work were selected to demonstrate the types of response found in MWTA when performing Mode 1 and Mode 2 experiments.

3.1. Mode 1 MWTA experiments (constant applied microwave power)

3.1.1. Effect on the temperature–time profile of materials with different loss factor using iron(II, III) oxide and alumina mixtures

The considerable effect of different loss factors on the temperatures attained by a material exposed to a constant microwave power is illustrated in Fig. 4 with the temperature profiles for three 2.7 g samples heated in a silica cell (Cell A, Fig. 3a) using a forward power of 185 W.

Temperature profile (a) was obtained from a 2.7 g sample of pure alumina which, under the experimental conditions used, only attained a temperature of ca. 160°C after 10 min with final heating rate approaching zero. Profile (b) reveals the dramatic effect of the addition of 0.1 g of iron(II, III) oxide (Fe_3O_4), a strong absorber of microwave energy [19], to 2.6 g of the alumina to give a sample of constant mass. Here, the temperature rose to 300°C in approximately 4 min with the final heating rate being in excess of 30°C min^{-1}. Increasing the fraction of Fe_3O_4 to 0.3 g produced an even more rapid temperature rise, as shown in profile (c).

3.1.2. Effect on the temperature–time profile produced by an increase in loss factor during the phase change in potassium nitrate

The effect of a change in loss factor on the temperature profiles obtained under constant applied power is illustrated by the solid–solid phase change in potassium nitrate (Aldrich, AnalaR) in Fig. 5. Three temperature profiles are shown, each for a 3.5 g mixture of 90% potassium nitrate with 10% silicon carbide (added to increase the overall loss factor of the mixture) contained in Cell A (Fig. 3a).

Profiles (a) to (c) show the temperature response of the sample for constant applied powers of 150, 143 and 135 W, respectively. As would be expected, the rate of temperature rise increases with increasing applied power. However, the temperature profiles are no longer featureless (as with the alumina sample shown in Fig. 4) but each shows a discontinuity at approximately 130°C, corresponding to the phase change [20], with a subsequent increase in heating rate. These profiles not only reveal the presence of the phase change and the temperature at which it occurs but also the fact that the high temperature phase is more lossy (i.e. couples more strongly with the microwave energy) than the low temperature phase.

A dotted line representing 130°C is shown in Fig. 5. This line indicates that the shift in temperature observed for the phase change, despite the very large sample and the considerable variation in heating rate, is only 4–5°C suggesting that reasonably uniform

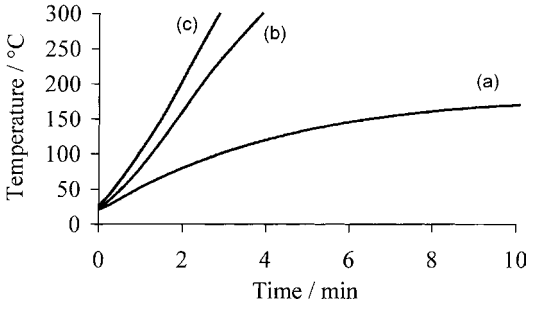

Fig. 4. Temperature–time profiles (Mode 1 experiments) for mixtures of Fe_3O_4 and alumina (2.7 g total mass) heated using a constant applied power of 185 W. (a) Alumina only; (b) 0.1 g Fe_3O_4; (c) 0.3 g Fe_3O_4.

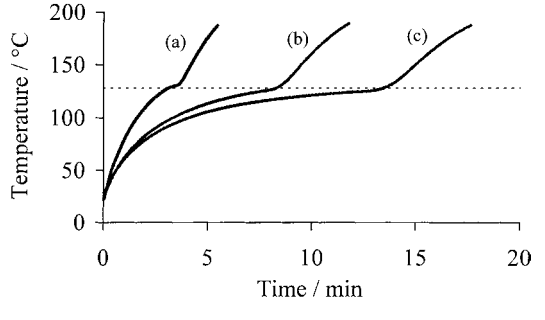

Fig. 5. Temperature–time profiles (Mode 1 experiments) obtained for a series of constant power experiments on 3.5 g of a mixture of 90% potassium nitrate and 10% silicon carbide. (a) 150 W; (b) 143 W; (c) 135 W.

heating of the sample was achieved. The reproducibility of the detection of the phase change demonstrates the potential of the technique for qualitative analysis.

3.1.3. Illustration of the quantitative use of time–temperature profiles using the phase change in potassium nitrate

It has been found that the time–temperature profile can be used quantitatively, as well as qualitatively, by measuring the time taken for the sample to heat between two temperatures. This is demonstrated using the phase change in potassium nitrate described above.

In this series of experiments the potassium nitrate was mixed with an inert diluent, potassium chloride, to give samples of the same mass and volume. Fig. 6 shows the temperature profiles for three such samples: 3 g of potassium nitrate (profile a), 1.5 g of potassium nitrate mixed with 1.5 g of potassium chloride (profile b) and 3 g of potassium chloride (profile c). All samples were run in Cell A and subjected to a constant applied power of 135 W.

The phase change at 130°C is clearly evident on profiles (a) and (b), while the featureless nature of profile (c) demonstrates that potassium chloride undergoes no thermal transitions in this temperature range.

The quantitative use of such data is shown in Fig. 7 in which the results of a series of experiments on a range of 3 g potassium nitrate/potassium chloride mixtures, using the conditions described above are plotted. The profile shows the log of the time taken for the temperature to rise from 25 to 125°C (i.e. prior to the phase change) plotted as a function of mass of potassium nitrate present.

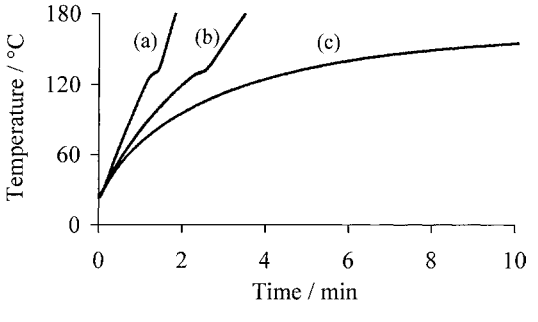

Fig. 6. Temperature–time profiles (Mode 1 experiments) obtained for a series of potassium nitrate and potassium chloride mixtures using a forward power of 135 W. (a) 3 g potassium nitrate; (b) 1.5 g potassium nitrate; (c) pure potassium chloride.

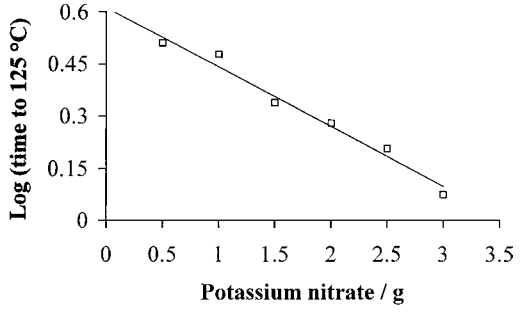

Fig. 7. Plot of the log of the time for the temperature to rise from 25 to 125°C for a series of potassium nitrate and potassium chloride mixtures heated using a forward power of 135 W.

It can be seen that there is a linear relationship (r^2=0.985) with greater masses of potassium nitrate producing faster heating rates, as expected. It is interesting to note that the results provide a quantitative measure of the amount of potassium nitrate present *without* any physicochemical change occurring in the sample. This suggests that the method could be applied to quantify materials that are thermally inert, although it would not discriminate between the contributions to the overall loss factor of a sample if three, or more, materials were present in differing quantities.

3.2. Mode 2 experiments (linear heating)

3.2.1. Effect on the power–time profile of materials with different loss factor using iron(II, III) oxide and alumina mixtures

The applied power and linear temperature profiles obtained from heating 2.7 g of alumina in Cell A at 5°C min^{-1} to 150°C and then cooling at 5°C min^{-1} to 50°C is shown in Fig. 8. It can be seen that, after an initial lag while the power rises to a level sufficient to heat the sample, good linear heating can be obtained. The power profile is relatively smooth and featureless (the sample being inert), with the step at around 28 min corresponding to the transition from heating to cooling.

The applied power profiles obtained for a series of three linear heating experiments (+5°C min^{-1} to 150°C then −5°C min^{-1} to 50°C) using 2.7 g samples of alumina (profile a), 2.6 g of alumina with 0.1 g

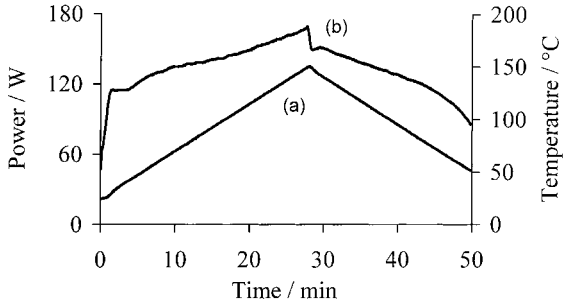

Fig. 8. (a) Temperature and (b) associated power profiles (Mode 2 experiment) for 2.7 g alumina heated at 5°C min^{-1} to 150°C, then cooled at −5°C min^{-1} to 50°C.

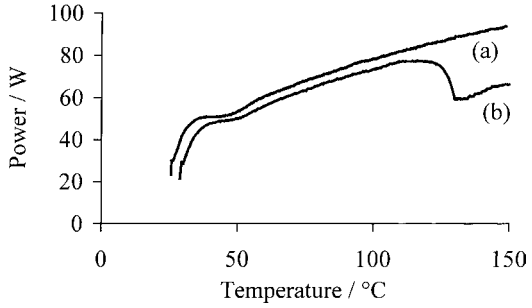

Fig. 10. Power profiles obtained for two linear heating experiments at 5°C min^{-1} (Mode 2 experiments). (a) 150 mg of silicon carbide; (b) mixture of 30 mg of benzilic acid with 120 mg of silicon carbide showing Type I event.

Fe_3O_4 (profile b) and 2.4 g of alumina with 0.3 g Fe_3O_4 (profile c) are shown in Fig. 9. It can be seen that the three profiles are very similar in general shape but, in agreement with the comparable constant power experiments shown in Fig. 4 above, less power is required to heat the samples containing the iron oxide because of its greater loss factor.

3.2.2. *Effect on the power–time profile of the melting of benzilic acid*

The shape of the applied power profile also provides a means of obtaining qualitative information. Fig. 10 shows the applied power profiles, plotted as a function of temperature, for two experiments using Cell B (Fig. 3b). Profile (a) is for 150 mg of silicon carbide while profile (b) is for 150 mg of a mixture of 30 mg of benzilic acid (Aldrich) and 120 mg of silicon carbide, both heated at 5°C min^{-1} to 150°C.

Profile (a) shows an initial rise in the applied power from its starting value of 20 W as the instrument attains the required level to attain the set heating rate. By 40°C linear heating has been achieved and the power profile is subsequently smooth and featureless, with a slow increase being all that is required to maintain 5°C min^{-1}. Profile (b), which has been slightly offset for clarity, shows a typical Type I power profile for the melting. The profile is virtually identical to that of the pure silicon carbide until around 135°C when the power drops by approximately 20 W, caused by an increase in the loss factor of the sample as the benzilic acid melts. Subsequently the power profile increases in parallel to that of profile (a), but at a lower underlying value. It is interesting to note that the melting event appears at a temperature approximately 15°C lower than is obtained conventionally. This effect is repeatable and has been observed for several materials that undergo an increase in loss factor on melting, as well as by other workers [10]. Although the cause of this apparent lowering of the melting point is still under investigation, one possibility is that small nuclei of molten material appear at a lower temperature than that of the bulk melt and it is these that cause the increase in loss factor.

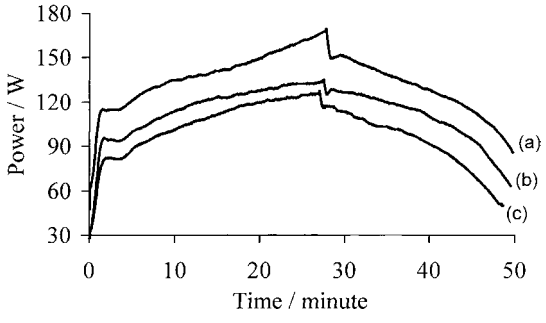

Fig. 9. Power profiles obtained for mixtures of Fe_3O_4 and alumina (2.7 g total mass) using linear heating of 5°C min^{-1} (Mode 2 experiments). (a) alumina only; (b) 0.1 g Fe_3O_4; (c) 0.3 g Fe_3O_4.

3.2.3. *Effect on the power–time profile of the melting of caffeine*

The high sensitivity of the applied power profile in MWTA in the detection of transitions is demonstrated by the melting of caffeine. Fig. 11 shows the applied power, plotted as a function of temperature, for a mixture of 2 mg of caffeine with 150 mg of silicon carbide, heated at 5°C min^{-1} in Cell B. At 230°C there is a very sharp drop in the power profile of nearly 40 W

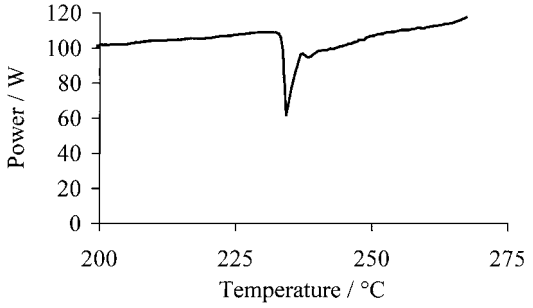

Fig. 11. Power profile obtained for a mixture of 2 mg of caffeine and 150 mg of silicon carbide heated at 5°C min^{-1} (Mode 2 experiment) showing Type II event.

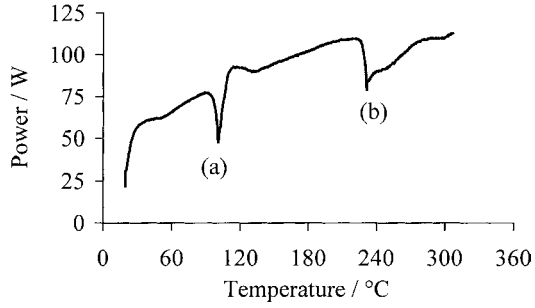

Fig. 13. Power profile obtained for a mixture of 20 mg of zinc acetate and 130 mg of silicon carbide heated at 10°C min^{-1} (Mode 1 experiment) showing a Type II and a complex Type I event.

as the caffeine melts (cf. 235°C quoted by the suppliers [21]), followed by a return to a level approximately 20 W lower than immediately prior to the melting typical of a Type II event. The power slowly rises subsequently as the molten caffeine is lost through volatilisation. As with the benzilic acid (Section 3.2.2) there appears to be a small lowering of the melting temperature, in this instance of approximately 5°C. Nevertheless, the technique clearly provides information which can be used for qualitative analysis.

3.2.4. Effect on the power–time profile of the complex decomposition of zinc acetate dihydrate

The use of applied power profile in the qualitative study of more complex systems is demonstrated by the decomposition of zinc acetate dihydrate.

The decomposition of a 10 mg sample of zinc acetate dihydrate heated at 10°C min^{-1} to 350°C in static air using conventional thermogravimetry (STA 625, Stanton Redcroft) is shown in Fig. 12. The

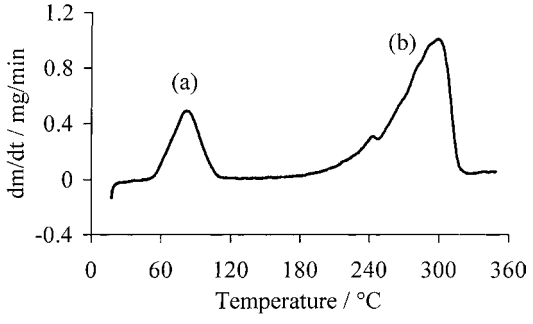

Fig. 12. Derivative of the mass loss profile for 10 mg of zinc acetate heated at 10°C min^{-1} using a conventional thermogravimetric analyser.

processes that occur in this temperature range produce two peaks when the derivative of the mass loss is plotted as a function of temperature. The first peak (a) is caused by the loss of water of crystallisation, while the second peak (b) results from the initial decomposition stage of the acetate itself.

The result of a comparable MWTA experiment is shown in Fig. 13. This gives the applied power profile, plotted as a function of temperature, produced by a 20 mg sample of zinc acetate mixed with 130 mg of silicon carbide and heated at 10°C min^{-1} to 350°C in Cell B. Again, two main events are clearly seen. The first event, (a), is primarily Type II in nature with the negative peak in the power profile caused by either the presence of some liquid water, or a transition state with a high loss factor. As the water of crystallisation is lost the power level rises again and maintains a smooth profile until the second event (b) causes a second rapid drop in the applied power of approximately 25 W at 240°C. This event shows a combination of Type I and Type II features, suggesting complex multi-stage processes. Eventually the power returns to a level similar to that immediately prior to the event. This profile may be explained in terms of the melting of the anhydrous acetate followed by decomposition [22]. The molten phase has a higher loss factor resulting in the sharp drop in the power profile, but as this material is gradually lost through decomposition to produce (low loss factor) zinc oxide there is a corresponding rise in the power profile.

Interestingly, the sharp drop in power at approximately 240°C appears to correspond with the small event seen on the DTG profile in Fig. 11. This illustrates the different relative sensitivities of these

two techniques which arise from the different parameters involved.

3.2.5. Effect on the power–time profile of the solid–solid phase in potassium perchlorate at different heating rates

As with all thermal analysis techniques, the magnitude of the response of MWTA is dependent on the heating rate. This is demonstrated with the phase change in potassium perchlorate which occurs at 300°C. Fig. 14 shows a series of applied power profiles for the heating of a 200 mg sample of potassium perchlorate using Cell B for heating rates of 2, 10, 20 and 30°C min^{-1} (profiles a to d, respectively).

It can be seen that, up to 300°C, all the applied power profiles are smooth, with faster heating rates naturally requiring a greater underlying power. The power follows a Type III profile for the phase change, though the magnitude of the response to the phase change increases with increasing heating rate, being indiscernible at 2°C min^{-1} and over 100 W at 30°C min^{-1}. For the 10°C min^{-1} experiments (profile b) the complex peak is roughly symmetrical, with the applied power being approximately the same immediately before and after the phase change. For the 20°C min^{-1} experiment (profile c) the final power level is slightly lower, and for the 30°C min^{-1} experiment (profile d) the asymmetry of the two peaks is pronounced, with the final power level being markedly less than the pre-phase change level. The cause of this profile shape, which has been observed in other systems, requires further investigation but may result from a transitional state between the two phases with differing dielectric properties.

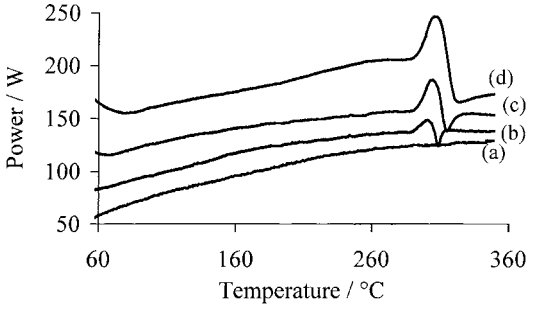

Fig. 14. Power profiles obtained for the heating of 200 mg of potassium perchlorate using a series of heating rates (Mode 2 experiments). The phase change appears as a Type III event. (a) 2°C min^{-1}; (b) 10°C min^{-1}; (c) 20°C min^{-1}; (d) 30°C min^{-1}.

In conventional thermal analysis faster heating rates often increase the sensitivity of the experiment. In the MWTA experiments it is possible that there is a slight change in loss factor between the high and low temperature phases of potassium perchlorate which becomes more apparent at the higher heating rates. Another commonly observed phenomenon in conventional thermal analysis is the apparent shift in temperature of an event with increasing heating rate. This shift arises from the temperature gradients generated across the sample as heat is transported to it (largely by conduction) from an external furnace. Only a very small shift in temperature is observed with the MWTA experiments (taking the temperature of the maximum of first peak in the power profile), suggesting that the uniformity of heating of the sample is good.

3.2.6. Quantitative measurements from the power–time profile using the phase change in potassium perchlorate

A series of experiments was carried out to investigate the relationship between the area of the positive peak component of the Type III profile and the mass of potassium perchlorate present.

For these experiments 3 g mixtures of potassium perchlorate and alumina were prepared containing 10, 25, 40, 50, 60 and 75% of the active component. These were heated at 10°C min^{-1} using Cell A and the area of the positive peak on the power profile determined by integration. Four separate experiments were performed on each mixture to give an indication of the repeatability of the method.

Fig. 15 shows the areas of the measured peaks plotted as a percentage of potassium perchlorate present. It can be seen that a linear relationship (r^2=0.974) exists over the mass range covered, demonstrating that the method is suitable for quantitative measurement. The spread of the values increases with peak area as would be expected, but the average deviation of 4.4 suggests reasonable repeatability between experiments on the same mass of potassium perchlorate.

A potential source of error in the results arises from the requirement to construct a baseline used to define the lower bound of the peak for integration. This can be difficult to achieve with complete certainty due to

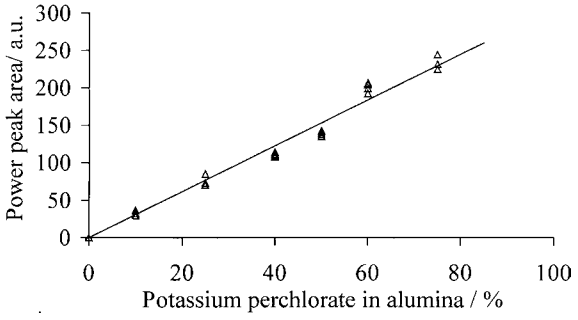

Fig. 15. Relationship between the percentage of potassium perchlorate in alumina and the area of the positive peak of the Type III response produced by the solid–solid phase change on heating a 3 g sample at 10°C min^{-1}.

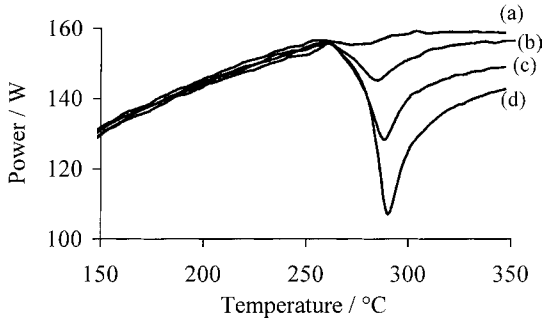

Fig. 16. Power profiles obtained for the heating of a series of 200 mg mixtures of basic copper carbonate in silicon carbide (Mode 2 experiments). The decomposition appears as a Type II event. (a) 10 mg; (b) 20 mg; (c) 40 mg; (d) 60 mg.

differences in the power level before and after the phase change. Similar difficulties can arise in the integration of peaks in conventional DSC when determining enthalpy values. Another source of error is that the larger active mass samples necessitated the greatest response in power and it was difficult to maintain absolute linearity of the heating rate through the process.

3.2.7. Quantitative measurements from the power–time profile using the decomposition of basic copper carbonate

That the magnitude of the change in the applied power during a thermal transition can provide quantitative information is further demonstrated using the decomposition of basic copper carbonate (Aldrich). This material decomposes to produce copper oxide [23], which has a high loss factor, with the evolution of carbon dioxide and water [24].

A series of experiments was performed on 200 mg mixtures of basic copper carbonate (10, 20, 30, 40, 50 and 60 mg) in silicon carbide using Cell B and a heating rate of 10°C min^{-1}. The resultant power profiles for these experiments (for clarity the profile for the 30 and 50 mg copper carbonate samples have been omitted) are shown in Fig. 16. The decomposition, starting around 270°C, produces an event which is primarily Type II in nature with the magnitude of negative peak increasing with mass of carbonate present in the sample. After the decomposition the applied power profiles rise again in all cases but, by 350°C, have returned to a baseline curve.

Accurate integration of the area of the peak is, again, difficult due to the uncertainty in the baseline. The level of the power profile after the decomposition also appears to decrease with increasing mass, but measurement of this requires the construction of an arbitrary baseline. For this work it was decided, therefore, to use the greatest value for the height as measured between the point immediately prior to the phase change to the minimum applied power level. A graph of these peak height values, plotted as a function of mass, produced a straight line (r^2=0.996) indicating a reasonable correlation between the applied power response and amount of sample present.

Experiments were performed also with sample masses above 60 mg. However, under the conditions used, these caused such large and rapid changes in the applied power that strict linear heating could not be maintained through the decomposition thus reducing the validity of the measurements.

4. Conclusions

The results presented in this paper demonstrate that MWTA can be used to detect a wide range of thermal transitions, including phase changes, melting and decompositions via changes in the material's ability to absorb microwave energy. This information can be found either from the temperature profile of the sample as it is subjected to a constant or pre-programmed power regime or from the applied power profile

required to force the sample to follow a linear temperature programme. Some of the results further suggest that MWTA can be a very sensitive technique, although this appears to be sample and process dependent.

To aid interpretation of MWTA results we have devised a simple classification of the changes in the power profile most commonly observed during thermal transitions. The temperature–time profiles (Mode 1 experiments) obtained using potassium nitrate suggest that it is possible to obtain quantitative measurements of the amount of a material present in a binary mixture purely from its effect on the total loss factor of the sample, even in the absence of any thermal transition.

The work on basic copper carbonate demonstrates that the power–time profiles (Mode 2 experiments) can also be used provide both qualitative and quantitative information. One problem is that there is no absolute 'baseline' against which to measure any deflections, making quantitative measurements difficult. To address this difficulty we are currently investigating modulated techniques where changes in the amplitude of the applied power required to induce a fixed amplitude sine wave on the temperature (superimposed upon an underlying linear heating rate) are used to detect thermal transitions. This approach has the advantage that, as amplitude is an absolute measurement, the need to determine or construct a baseline is eliminated.

Future work will be complemented by studies using more accurate sensors to measure both the forward and reflected power, so providing a more precise measure of the power adsorbed by the sample. To allow a more direct comparison between microwave and non-microwave heating under identical experimental conditions, a conventional furnace is being constructed that will be suitable to hold the sample cells used in the MWTA system. This arrangement will also permit the contribution of heat capacity and enthalpy for any given material to be determined.

References

[1] P. Monsef-Mirzai, M. Ravindran, R. McWhinnie, P. Burchill, Fuel 74 (1) (1995) 20.
[2] Y.-L. Tian, B.-S. Li, J.-L. Shi, K.-Z. Song, J.-K. Guo, J.-L. Tao, Chin. Sci. Bull. 36 (11) (1991) 900.
[3] M. Chen, J.W. Hellgeth, T.C. Ward, J.E. McGrath, Polym. Eng. Sci. 35 (2) (1995) 145.
[4] F.-S. Xiao, W. Xu, S. Qiu, R. Xu, J. Mater. Chem. 4 (5) (1994) 735.
[5] G. Bond, R. Moyes, S.D. Pollington, D.A Whan, in: L. Guczi (Ed.), New Frontiers in Catalysis, Elsevier, Amsterdam, 1993, p. 1805.
[6] K.G.K. Warrier, P. Mukundan, S.K. Ghosh, S. Sivakumar, A.D. Damodaran, J. Mater. Sci. 29 (1994) 3415.
[7] P.J. Jones, A.T. Rowley, Drying Technol. 14 (5) (1996) 1063.
[8] D.M.P. Mingos, D.R. Baghurst, Chem. Soc. Rev. 20 (1991) 1.
[9] E. Karmazsin, R. Barhoumi, P. Satre, J. Therm. Anal. 29 (1984) 1269.
[10] E. Karmazsin, Thermochim. Acta 110 (1987) 289.
[11] G.M.B. Parkes, P.A. Barnes, G. Bond, E.L. Charsley, Rev. Sci. Inst. (1999), in press.
[12] G.M.B. Parkes, P.A. Barnes, E.L. Charsley, G. Bond, Anal. Chem. (1999), in press.
[13] E. Karmazsin, R. Barhoumi, P. Satre, F. Gaillard, J. Therm. Anal. 30 (1985) 43.
[14] G.M.B. Parkes, P.A. Barnes, E.L. Charsley, G. Bond, J. Therm. Anal. Cal. 56 (1999) 723.
[15] T. Labuza, J. Meister, J. Microwave Power Electromag. Energy 27 (4) (1992) 205.
[16] J.G. Binner, J.A. Fernie, P.A. Whitaker, J. Mater. Sci. 33 (12) (1998) 3009.
[17] B.G. Ravi, P.D. Ramesh, N. Gupta, R.J. Rao, J. Mater. Chem. 7 (10) (1997) 2043.
[18] N.N. Greenwood, A. Earnshaw, Chemistry of the Elements, 2nd Edition, Butterworths, London, 1997.
[19] M. Ravindran, P. Monsefmirzai, J.K. Maund, W.R. McWhinnie, P. Burchill, J. Therm. Anal. 44 (1) (1995) 25.
[20] K. Kostyrko, M. Skoczylas, J. Therm. Anal. 38 (9) (1992) 2181.
[21] Catalogue Handbook of Fine Chemicals, Aldrich, 1997.
[22] X.Y. Zhao, B.C. Zheng, C.Z. Li, H.C. Gu, Powder Technol. 100 (1) (1998) 20.
[23] I.T. Kim, Y.H. Kim, Eur. J. Solid State In. Chem. 33 (10) (1996) 971.
[24] S.A.A. Mansour, J. Therm. Anal. 42 (6) (1994) 1251.